Published in final edited form as:
Nat Med. 2009 April ; 15(4): 442–446. doi:10.1038/nm.1937.

Deficiency of the intestinal enzyme acyl CoA:monoacylglycerol acyltransferase-2 protects mice from metabolic disorders induced by high-fat feeding

Chi-Liang Eric Yen[1,2,5], **Mei-Leng Cheong**[1], **Carrie Grueter**[1,2], **Ping Zhou**[1], **Junya Moriwaki**[1], **Jinny S Wong**[1], **Brian Hubbard**[3], **Stephen Marmor**[3], and **Robert V Farese Jr**[1,2,4]

[1] Gladstone Institute of Cardiovascular Disease, San Francisco, California, USA

[2] Cardiovascular Research Institute, University of California, San Francisco, California, USA

[3] Novartis Institutes for Biomedical Research, Cambridge, Massachusetts, USA

[4] Departments of Medicine, Biochemistry and Biophysics, University of California, San Francisco, California, USA

Abstract

Animals are remarkably efficient in absorbing dietary fat and assimilating this energy-dense nutrient into the white adipose tissue (WAT) for storage. Although this metabolic efficiency may confer an advantage in times of calorie deprivation, it contributes to obesity and associated metabolic disorders when dietary fat is abundant[1,2]. Here we show that the intestinal lipid synthesis enzyme acyl CoA:monoacylglycerol acyltransferase-2 (MGAT2) has a crucial role in the assimilation of dietary fat and the accretion of body fat in mice. Mice lacking MGAT2 have a normal phenotype on a low-fat diet. However, on a high-fat diet, MGAT2-deficient mice are protected against developing obesity, glucose intolerance, hypercholesterolemia and fatty livers. Caloric intake is normal in MGAT2-deficient mice, and dietary fat is absorbed fully. However, entry of dietary fat into the circulation occurs at a reduced rate. This altered kinetics of fat absorption apparently results in more partitioning of dietary fat toward energy dissipation rather than toward storage in the WAT. Thus, our studies identify MGAT2 as a key determinant of energy metabolism in response to dietary fat and suggest that the inhibition of this enzyme may prove to be a useful strategy for treating obesity and other metabolic diseases associated with excessive fat intake.

Dietary fat, as triacylglycerol, is a major source of calories, accounting for over 30% of daily intake in most developed countries[3]. The assimilation of triacylglycerol as body fat is remarkably efficient, owing in part to near complete absorption in the small intestine. Intestinal fat absorption involves hydrolysis of dietary triacylglycerol to monoacylglycerol and fatty acids in the lumen, lipid uptake by enterocytes of the proximal small intestine, resynthesis of triacylglycerol and triacylglycerol incorporation into chylomicrons for distribution to tissues. The probable rate-limiting step of triacylglycerol synthesis is formation of diacylglycerol from monoacylglycerol and fatty acyl CoA substrates, catalyzed by MGAT[4,5]. The MGAT pathway

Correspondence should be addressed to R.V.F. Jr. (bfarese@gladstone.ucsf.edu).
[5]Current address: Department of Nutritional Sciences, University of Wisconsin–Madison, Madison, Wisconsin, USA.

Note: Supplementary information is available on the Nature Medicine website.

AUTHOR CONTRIBUTIONS

C.-L.E.Y. designed and conducted experiments, coordinated the project and co-wrote the manuscript; M.-L.C., J.M., C.G., P.Z. and J.S.W. performed phenotyping experiments; B.H. and S.M. performed hormone assays; R.V.F. Jr directed the project and co-wrote the manuscript.

accounts for ~75% of triacylglycerol synthesis in the intestine; the remainder is presumably mediated by the glycerol-3-phosphate pathway[6,7]. Of three identified MGAT enzymes[8–11], MGAT2 and MGAT3 are expressed in the small intestine. MGAT2 is highly expressed in the proximal small intestine in both humans and mice, whereas human MGAT3 expression is highest in the distal intestine (the gene is apparently not expressed in mice)[9–11]. We found mouse *Mogat2* mRNA levels were highest in the small intestine; other tissues (for example, kidney, stomach, adipose tissues and liver) had <1% of that in the small intestine[9] (Supplementary Fig. 1 online). In the small intestine, *Mogat2* mRNA was present in enterocytes of intestinal villi, and levels doubled after high-fat feeding (Supplementary Figs. 1 and 2 online)[12].

To determine the requirement for MGAT2 in dietary fat absorption, we generated *Mogat2*$^{-/-}$ mice, which lack MGAT2 protein and have a greater than 50% decrease in intestinal MGAT activity compared with wild-type mice (Supplementary Fig. 2). *Mogat2*$^{-/-}$ mice were born at expected Mendelian frequencies with no apparent abnormalities. On a low-fat chow diet, they gained weight normally, and their body composition was similar to wild-type mice (Fig. 1). However, on a diet containing 60% calories from fat, male *Mogat2*$^{-/-}$ mice gained less than wild-type mice, and *Mogat2*$^{+/-}$mice had an intermediate phenotype (Fig. 1b). After 16 weeks, *Mogat2*$^{-/-}$ mice weighed 40% less than did wild-type mice, and their fat mass was more than 50% lower (Fig. 1b,**c**). Lean body mass and body length (data not shown) were similar in mice of both genotypes. Decreased weight gain was also observed in female *Mogat2*$^{-/-}$ mice fed the 60% high-fat diet (Fig. 1d) and in male *Mogat2*$^{-/-}$ mice fed a diet with 45% calories from fat (Supplementary Fig. 3 online). Thus, MGAT2 deficiency protects against obesity caused by a high-fat diet. We did not examine whether MGAT2 deficiency protects against other causes of obesity, such as leptin deficiency, in this study.

Obesity is frequently accompanied by metabolic disorders that can be induced by high-fat diets. We examined whether *Mogat2*$^{-/-}$ mice were protected against these conditions. Male *Mogat2*$^{-/-}$ mice had lower fasting insulin concentrations and better glucose tolerance after prolonged high-fat feeding (Fig. 2). They also had lower fasting concentrations of total and non–high-density lipoprotein cholesterol in plasma (Fig. 2b); plasma triacylglycerol concentrations were similar in wild-type and *Mogat2*$^{-/-}$ mice (37.8 ± 1.9 mg dl^{-1} versus 32.3 ± 2.7 mg dl^{-1}, respectively). *Mogat2*$^{-/-}$ mice were also protected against hepatic steatosis (Fig. 2c), with hepatic triacylglycerol content being <5% of that in wild-type mice (6.0 ± 1.6 nmol per mg tissue versus 131 ± 10.5 nmol per mg tissue). Thus, MGAT2 deficiency protects mice from glucose intolerance, hypercholesterolemia and hepatic steatosis induced by a high-fat diet.

To investigate mechanisms underlying the striking phenotype of *Mogat2*$^{-/-}$ mice, we examined energy balance. Food intake was similar during 1 week of high-fat feeding, when *Mogat2*$^{-/-}$ mice gained less weight than wild-type mice (Fig. 3a), suggesting differences in energy expenditure. Oxygen consumption during the dark phase of the light cycle, when mice are awake and eating, was ~7% higher in *Mogat2*$^{-/-}$ mice fed a high-fat diet (Fig. 3b). Locomotor activity was not increased (Fig. 3c), suggesting that *Mogat2*$^{-/-}$ mice have higher resting metabolic rates, thermogenesis or both. Supporting this notion, their body temperatures on a high-fat diet were higher (Fig. 3d).

We next examined intestinal absorption of dietary fat. In studies using a nonabsorbable fat[13] as a reference, fat was absorbed at similarly high proportions in *Mogat2*$^{-/-}$ and wild-type mice, even when fat accounted for 60% of dietary calories (Fig. 4a). Fecal fat amounts were similar (6.5 ± 3.1 mg per mouse per day versus 8.4 ± 3.4 mg per mouse per day for wild-type and *Mogat2*$^{-/-}$ mice, respectively), as were fecal mass and energy content (Fig. 4b). Tissue stores of the fat-soluble vitamins A and E were also similar (Fig. 4c). Chylomicron-sized lipoprotein

particles appeared in the circulation of *Mogat2*$^{-/-}$ mice after an oral bolus of oil (Supplementary Fig. 4 online), indicating that *Mogat2* is not required for assembly and secretion of chylomicrons. Thus, dietary fat absorption is intact in *Mogat2*$^{-/-}$ mice, and normal quantities of fat are absorbed.

The normal dietary fat absorption in *Mogat2*$^{-/-}$ mice suggested that they can synthesize triacylglycerol in enterocytes. Indeed, triacylglycerol was the most abundant lipid in the small intestine of *Mogat2*$^{-/-}$ mice fed a high-fat diet, and monoacylglycerol, an MGAT2 substrate, did not accumulate in the small intestine (Fig. 4d). Additionally, acute administration of radioactive monoacylglycerol tracer into the intestinal lumen verified that, within 5 min, triacylglycerol was synthesized in enterocytes of *Mogat2*$^{-/-}$ mice in amounts 70% of wild-type levels (data not shown). We suspect intestinal triacylglycerol is synthesized in *Mogat2*$^{-/-}$ mice either by another MGAT enzyme[14], as there was residual activity converting monoacylglycerol to diacylglycerol and triacylglycerol (Supplementary Fig. 2d), or by breakdown of monoacylglycerol to glycerol and fatty acid, which enters the glycerol-phosphate pathway. The latter pathway would require more energy than the MGAT pathway and could contribute to the metabolic inefficiency of *Mogat2*$^{-/-}$ mice.

Because absorption of dietary fat was quantitatively normal in *Mogat2*$^{-/-}$ mice, we hypothesized that their lower propensity for obesity may involve a lower rate of absorption of dietary fat into the circulation. To test this, we examined the rate of triacylglycerol entry into the circulation after an intragastric bolus of olive oil. Plasma triacylglycerol concentrations increased transiently in wild-type but not *Mogat2*$^{-/-}$ mice (Supplementary Fig. 4b). After mice were orally given dietary oil containing ^{14}C-trioleoylglycerol (administered with tyloxapol, which blocks lipolysis in plasma), the radioactivity and triacylglycerol abundance in plasma accumulated more slowly in *Mogat2*$^{-/-}$ mice (Fig. 4e), confirming a reduced rate of fat entering the circulation.

Less fat absorption in the proximal small intestine of *Mogat2*$^{-/-}$ mice might result in more fat reaching the distal intestine. Indeed, we observed clusters of lipid droplets in enterocytes of the midintestine (jejunum) of *Mogat2*$^{-/-}$, but not wild-type, mice fed a high-fat diet (Fig. 4f). Oral dosing of a ^{14}C-trioleoylglycerol yielded smaller amounts of labeled lipids in the midintestine and larger amounts in the distal intestine of *Mogat2*$^{-/-}$ mice compared to wild-type mice (Fig. 4g). Also, amounts of postprandial glucagon-like peptide-1 (GLP-1), an incretin peptide released by the distal gut in response to nutrients[15], were larger in *Mogat2*$^{-/-}$ mice chronically fed a high-fat diet, whereas peptide YY (PYY) levels were similar (Fig. 4h).

Our data suggest that MGAT2 deficiency diminishes fat uptake in the proximal small intestine and delays fat entry into the circulation, changing the spatiotemporal distribution of fat absorption in the intestine when dietary fat consumption is high. This process may dissociate fat from carbohydrate absorption and insulin secretion and may result in reduced fat storage, enhanced fat oxidation and metabolic inefficiency. How MGAT2 deficiency triggers thermogenesis is unclear. We excluded several mechanisms. Increased fat oxidation in the small intestine of *Mogat2*$^{-/-}$ mice is unlikely, as mRNA expression of genes involved in fat oxidation showed no differences between genotypes (Supplementary Fig. 5a online). In rodents, thermogenesis is often mediated by brown adipose tissue (BAT) and uncoupling protein-1 (UCP-1)[16]. However, *Ucp1* mRNA levels were not increased in BAT of *Mogat2*$^{-/-}$ mice (Supplementary Fig. 5b), and BAT masses were similar (data not shown). BAT of *Mogat2*$^{-/-}$ mice fed a high-fat diet was darker and contained fewer lipid droplets than that of wild-type mice, consistent with increased fat oxidation. Also, plasma concentrations of thyroid hormones were normal in *Mogat2*$^{-/-}$ mice (data not shown).

We suspect that the delayed fat absorption in *Mogat2*$^{-/-}$ mice results in the partitioning of more dietary fat to BAT or other tissues, where it is oxidized. Greater flux would increase uncoupling-mediated thermogenesis in BAT. *Ucp2* mRNA levels in BAT were markedly increased (Supplementary Fig. 5b), perhaps reflecting greater oxidative stress from increased flux of substrates[17]. Increased flux could also promote uncoupling directly through the ability of fatty acids to promote this process[17]. Delayed fat absorption, with more fat reaching the distal intestine, may also trigger gut-derived neuroendocrine responses that promote fat burning over accretion. Although GLP-1 concentrations were increased in the plasma of *Mogat2*$^{-/-}$ mice, this is not a likely mechanism: administering exendin-3(9–39), a GLP-1 receptor antagonist, did not alter body weight (data not shown), and mice lacking the GLP-1 receptor had no changes in body weight[18].

We identified MGAT2 as a key determinant of energy metabolism in response to dietary fat. These findings may be relevant to human obesity: MGAT2 is expressed in human small intestine[9,10], and three microsatellite loci markers encompassing human *MOGAT2* on chromosome 11q13.5 are associated with altered resting energy expenditure, whereas one is linked to body-fat percentage[19]. Thus, variations in *MOGAT2* expression may contribute to differences in metabolic efficiency and propensity to weight gain in humans consuming diets rich in fat. Our findings also suggest that inhibiting MGAT2 in the small intestine might be useful for treating metabolic diseases caused by excessive fat intake. Attempts to block fat digestion in the intestinal lumen has had limited success in the clinic. Given our findings, the intracellular enzyme MGAT2 seems to be uniquely positioned as a possible intestinal target for interfering with fat absorption.

METHODS

Generation of *Mogat2*-deficient mice

We generated *Mogat2*-targeted 129/SvJae embryonic stem cells and, subsequently, mice carrying this mutation with a targeting vector designed to replace exon 1 of *Mogat2*, including the translation-initiating methionine, with a neomycin-resistance cassette. We confirmed *Mogat2* disruption by Southern blotting of genomic DNA that had been digested with *Bst*XI with a probe hybridizing upstream of sequences included in the targeting vector and by PCR (described in Supplementary Fig. 2a). We generated *Mogat2*$^{-/-}$ and wild-type littermates from breeding heterozygotes (that were first backcrossed for 10–12 generations with C57BL/6J mice from the Jackson Laboratory) and housed them in a pathogen-free facility. Diets were standard chow, containing 11.9% calories from fat (5053 PicoLab; Purina), or semipurified diets containing 10%, 45% or 60% calories from fat (Research Diets). The University of California–San Francisco Institutional Animal Care and Use Committee approved all procedures involving mice.

Body weight, composition and temperature

To monitor long-term growth, we weaned mice at 3 weeks of age onto the standard chow diet, weighed them weekly between 16:00 and 18:00 and kept them on the low-fat chow or switched them to the 60% high-fat diet at 9 weeks of age. We analyzed body composition by dual-energy X-ray absorptiometry (DEXA) with a PixiMus2 scanner (GE Healthcare Lunar) after a 4-h fast, and we measured body lengths from nose tip to tail base after anesthesia. For monitoring food intake and weight gain in home cages, we acclimatized adult mice to individual caging and to the high-fat diet for a week, weighed them and their food daily and pooled the data for the following 7 d. We measured core body temperature rectally with a digital thermometer (model 4600; Yellow Springs Instruments) between 14:00 and 16:00 after deprivation of food for 4 h (fast) and between 21:00 and 22:00 (*ad libitum*; fed).

Biochemical assays

We measured plasma triacylglycerol, total cholesterol, HDL-cholesterol, insulin, GLP1 (active), and PYY (total) levels by enzymatic assay or enzyme-linked immunoassay kits (triacylglycerol, Trig/GB, Roche/Hitachi Diagnostics; cholesterol, Waco Chemicals; insulin, Crystal Chem; GLP1, Millipore; PYY, Diagnostic Systems Laboratories). For GLP1 and PYY, we collected plasma 2 h after feeding and immediately added a dipeptidyl peptidase IV inhibitor (Millipore). We sent samples to Craft Technologies to measure retinol, retinyl esters and α-tocopherol. We measured MGAT activity and tissue triacylglycerol as previously described[8, 20]. We visualized lipids by iodine vapor or by dipping the plate into a solution of 10% cupric sulfate and 8% phosphoric acid and heating to 180 °C. We quantified rriacylglycerol mass was quantified by a previously described method4, with triolein as a standard.

Absorption of dietary fat

We assessed fat absorption during chronic high-fat feeding and after an acute challenge with a bolus of oil. We measured triacylglycerol absorption during high-fat feeding first using the fat balance assay developed by the Mouse Phenotyping Center at the University of Cincinnati[13]. We collected feces from mice fed diets containing the nonabsorbable fat sucrose polybenehate and 60% calories from lard. We calculated fat absorption from the ratios of behenic acid to other fatty acids in diet and feces. We next determined the fat contents of the diet and feces by weight. We monitored food intake and fecal output in individually caged mice fed a high-fat (60%) diet over a six-day period. We dried, weighed and ground a portion of diet and collected feces, extracted each with 40 ml of chloroform:methanol (2:1), and weighed lipid residues after the solvents were evaporated. We determined the caloric content of feces with an adiabatic bomb calorimeter (1241 Oxygen Bomb Calorimeter; Parr Instrument Company). For acute studies, we measured plasma triacylglycerol concentrations before (time 0) we had challenged mice with a bolus of 200 μl of olive oil through intragastric gavage and at 1 h, 2 h and 4 h after the challenge. To inhibit the clearance of plasma triacylglycerol, we administered 100 μl of the surfactant tyloxapol (5% in PBS, Sigma) through a tail vein. After 15 min, we collected blood before (time 0) and at 1 h, 2 h and 4 h after we had challenged mice with 200 μl of olive oil containing 2 μCi ^{14}C-trioleoylglycerol for triacylglycerol measurement and scintillation counting. To visualize chylomicron-size lipoprotein particles, we pooled plasma fractions from 1-h samples, ultracentrifuged them and examined the particles floating on the surface layer (density < 1.006 g ml^{-1}) by electron microscopy after negative staining with potassium phosphotungstate[20].

Distribution of dietary fat uptake

We assessed the uptake of dietary fat along the length of the small intestine by modifying a previously described method[21]. We fasted the mice for 4h and gavaged them with 1 μCi of ^{14}C-trioleoylglycerol in 100 μl of olive oil. Two hours later, we excised the small intestine (between the base of the stomach and the cecal junction), flushed it with 0.5 mM sodium taurocholate in PBS and cut it into 2-cm segments. We digested each segment with 500 μl of 1 N NaOH at 65 °C for 1 h, mixed it with 5 ml of Hionicfluor liquid scintillation cocktail (PerkinElmer) and measured counts per minute with a scintillation counter.

Energy balance

We measured oxygen consumption and physical activity by a monitoring system (Oxymax; Columbus Instruments) after mice were acclimated to the system and various diets under the regular 12-h light-dark cycle. We took measurements from each cage about every 15 min, and we performed experiments for 3 d per diet condition. We separated the data on the basis of light-dark cycle, pooled and averaged them. We normalized oxygen consumption data to lean body mass, as measured by DEXA scanning on the day before calorimetry studies.

Statistical analyses

We compared means of two groups by the *t* test for parametric data and the Mann-Whitney rank sum test for nonparametric data. When we compared more than two groups, we performed analysis of variance followed by *post hoc* tests. For most experiments, we performed two-way analysis of variance to determine whether the effects of genotype and diet were significant; if so, we performed Bonferroni post-tests for group comparisons.

Supplementary Material

Refer to Web version on PubMed Central for supplementary material.

Acknowledgments

We thank R. Jandacek at the University of Cincinnati Mouse Phenotyping Center for measuring lipid absorption; J.D. Fish for histological assistance; D. Walker for assistance with *in situ* hybridizations; D. Dubiel and K. Veenstra for measuring PYY and GLP-1; R. Bituin for mouse husbandry; Q. Walker for blastocyst microinjections; S. Ordway and G. Howard for editorial assistance; D. Jones for manuscript preparation; members of the Farese laboratory, M. Hirschey and M. Brown for insightful discussions; and R. Mahley and D. Srivastava for comments on the manuscript. This work was supported by funding from the American Heart Association (Scientist Development Grant to C.-L.E.Y.), the US National Institutes of Health (DK-056084 to R.V.F. Jr.), the US National Center for Research Resources (C06 RR018928), and the J. David Gladstone Institutes.

References

1. Neel JV. Diabetes mellitus: a ‘thrifty’ genotype rendered detrimental by ‘progress’? Am J Hum Genet 1962;14:353–362. [PubMed: 13937884]
2. Muoio DM, Newgard CB. Obesity-related derangements in metabolic regulation. Annu Rev Biochem 2006;75:367–401. [PubMed: 16756496]
3. The Food and Agricultural Organization of the United Nations. Food Consumption: Dietary Energy, Protein and Fat. 2008. http://www.fao.org/faostat/foodsecurity/index_en.htm
4. Bell RM, Coleman RA. Enzymes of glycerolipid synthesis in eukaryotes. Annu Rev Biochem 1980;49:459–487. [PubMed: 6250446]
5. Senior JR, Isselbacher KJ. Direct esterification of monoglycerides with palmityl coenzyme A by intestinal epithelial subcellular fractions. J Biol Chem 1962;237:1454–1459. [PubMed: 13910673]
6. Kayden HJ, Senior JR, Mattson FH. The monoglyceride pathway of fat absorption in man. J Clin Invest 1967;46:1695–1703. [PubMed: 6061744]
7. Mattson FH, Volpenhein RA. The digestion and absorption of triglycerides. J Biol Chem 1964;239:2772–2777. [PubMed: 14216426]
8. Yen CLE, Stone SJ, Cases S, Zhou P, Farese RV Jr. Identification of a gene encoding MGAT1, a monoacylglylcerol acyltransferase. Proc Natl Acad Sci USA 2002;99:8512–8517. [PubMed: 12077311]
9. Yen CLE, Farese RV Jr. MGAT2, a monoacylglycerol acyltransferase expressed in the small intestine. J Biol Chem 2003;278:18532–18537. [PubMed: 12621063]
10. Cao J, Lockwood J, Burn P, Shi Y. Cloning and functional characterization of a mouse intestinal acyl-CoA:monoacylglycerol acyltransferase, MGAT2. J Biol Chem 2003;278:13860–13866. [PubMed: 12576479]
11. Cheng D, et al. Identification of acyl coenzyme A:monoacylglycerol acyltransferase 3, an intestinal specific enzyme implicated in dietary fat absorption. J Biol Chem 2003;278:13611–13614. [PubMed: 12618427]
12. Cao J, et al. A predominant role of acyl-CoA:monoacylglycerol acyltransferase-2 in dietary fat absorption implicated by tissue distribution, subcellular localization, and up-regulation by high fat diet. J Biol Chem 2004;279:18878–18886. [PubMed: 14966132]
13. Jandacek RJ, Heubi JE, Tso P. A novel, noninvasive method for the measurement of intestinal fat absorption. Gastroenterology 2004;127:139–144. [PubMed: 15236180]

14. Yen CLE, Monetti M, Burri BJ, Farese RV Jr. The triacylglycerol synthesis enzyme DGAT1 also catalyzes the synthesis of diacylglycerols, waxes, and retinyl esters. J Lipid Res 2005;46:1502–1511. [PubMed: 15834126]
15. Baggio LL, Drucker DJ. Biology of incretins: GLP-1 and GIP. Gastroenterology 2007;132:2131–2157. [PubMed: 17498508]
16. Lowell BB, Spiegelman BM. Towards a molecular understanding of adaptive thermogenesis. Nature 2000;404:652–660. [PubMed: 10766252]
17. Krauss S, Zhang CY, Lowell BB. The mitochondrial uncoupling-protein homologues. Nat Rev Mol Cell Biol 2005;6:248–261. [PubMed: 15738989]
18. Scrocchi LA, et al. Glucose intolerance but normal satiety in mice with a null mutation in the glucagon-like peptide 1 receptor gene. Nat Med 1996;2:1254–1258. [PubMed: 8898756]
19. Bouchard C, Pérusse L, Chagnon Y, Warden C, Ricquier D. Linkage between markers in the vicinity of the uncoupling protein 2 gene and resting metabolic rate in humans. Hum Mol Genet 1997;6:1887–1889. [PubMed: 9302267]
20. Snyder F, Stephens N. A simplified spectrophotometric determination of ester groups in lipids. Biochim Biophys Acta 1959;34:244–245. [PubMed: 13832326]
21. Hamilton RL Jr, Goerke J, Guo LSS, Williams MC, Havel RJ. Unilamellar liposomes made with the French pressure cell: A simple preparative and semiquantitative technique. J Lipid Res 1980;21:981–992. [PubMed: 7193233]
22. Iqbal J, Hussain M. Evidence for multiple complementary pathways for efficient cholesterol absorption in mice. J Lipid Res 2005;46:1491–1501. [PubMed: 15834127]
23. Cases S, et al. Cloning of DGAT2, a second mammalian diacylglycerol acyltransferase, and related family members. J Biol Chem 2001;276:38870–38876. [PubMed: 11481335]

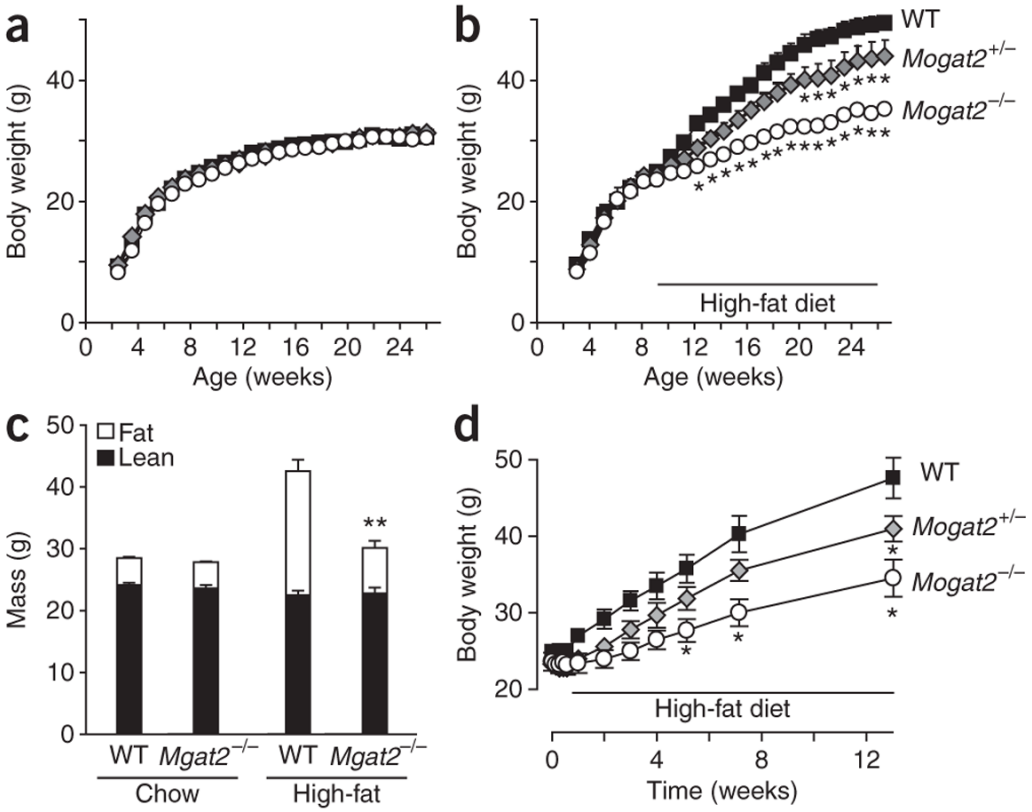

Figure 1.

MGAT2-deficient mice are protected from obesity induced by high-fat feeding. (**a**,**b**) Growth curves of male mice on a regular diet (10% calories from fat; **a**) or switched to a high-fat diet (60% calories from fat; underlined; **b**) at 9 weeks of age. $n = 8–16$ mice per group. $^{*}P < 0.01$ versus wild type. (**c**) Body composition of 5–6-month-old male mice, as determined by DEXA. $n = 12–16$ mice per group. $^{**}P < 0.001$ versus wild type fat mass. (**d**) Weight gain of 4–6-month-old female mice fed a regular diet and then switched to a high-fat diet (underlined) for 12 weeks. $n = 8$ mice per group. $^{*}P < 0.01$ versus wild type. Values are means ± s.e.m.

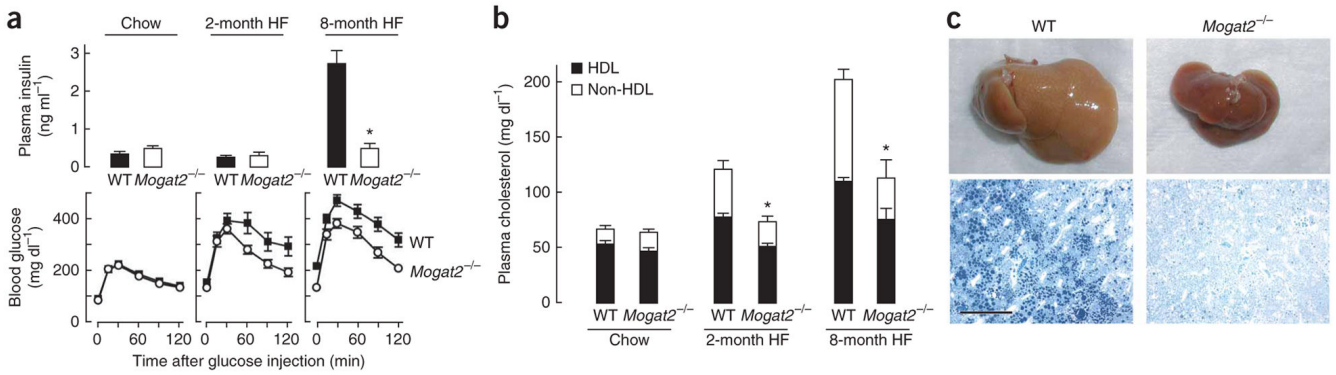

Figure 2.

MGAT2-deficient mice are protected from metabolic disorders induced by high-fat feeding. (**a**) Protection from hyperinsulinemia and glucose intolerance. Fasting plasma insulin (top) and blood glucose concentrations (bottom) of 8–11-month-old male wild-type and *Mogat2*$^{-/-}$ mice fed chow (n = 6 and 10, respectively), a high-fat diet for 2 months (n = 9 per group), or a high-fat diet for 7–9 months (8-month HF, n = 13 and 12, respectively) after an intraperitoneal injection of glucose (1 mg per g body weight). (**b**) Protection from hypercholesterolemia. Plasma cholesterol concentrations of mice fasted for 4 h. Solid bars represent high-density lipoprotein (HDL) cholesterol (same number of mice per group as in **a**). (**c**) Protection from hepatic steatosis. Representative appearance (top) and osmium tetroxide–toluidine blue–stained sections (bottom) of livers from wild-type and *Mogat2*$^{-/-}$ mice fed a high-fat diet for 7–8 months. Scale bar, 100 μm. Values are means ± s.e.m. *P < 0.01 versus wild type.

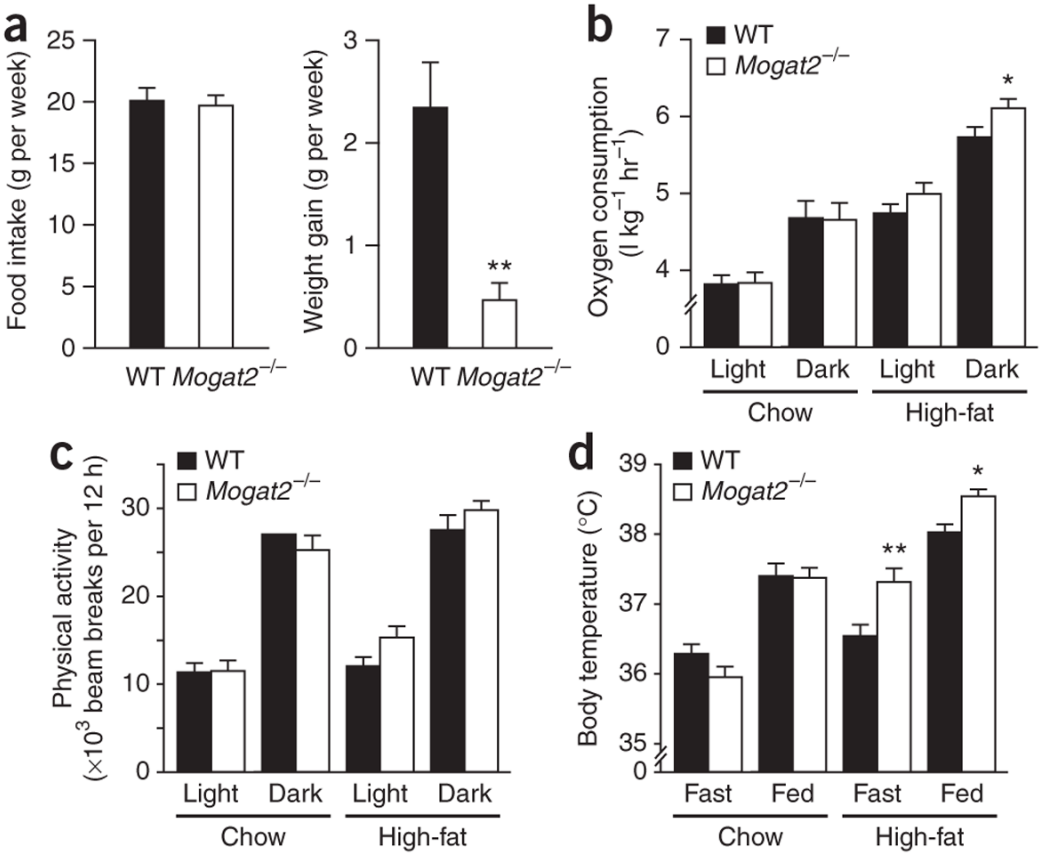

Figure 3.

MGAT2-deficient mice show increased energy expenditure and body temperature. (**a**) Food intake in wild-type and *Mogat2*$^{-/-}$ mice. Cumulative food intake (left) and weight gain (right) of adult male mice (6–7 months old) during a 1-week period after being acclimated to individual housing and a 60% high-fat diet for a week. wild-type, $n = 15$; *Mogat2*$^{-/-}$, $n = 11$. (**b**) Oxygen consumption in wild-type and *Mogat2*$^{-/-}$ mice. Male mice (5–6 months old) were acclimated individually in metabolic cages, and experiments were performed for 3 d on 10% fat (chow) or 60% fat (high-fat) diet. Data were normalized by lean body mass and were averages of light or dark phases from 3-day measurements. $n = 12$ per group. (**c**) Levels of physical activity in wild-type and *Mogat2*$^{-/-}$ mice. Activity was assessed by breaks of light beams, and experiments were performed as described in **b**. (**d**) Body temperature in wild-type *Mogat2*$^{-/-}$ mice fed the indicated diet under fasted or fed condition. $n = 12$–25 mice per group. Values are means ± s.e.m. *$P < 0.01$ and **$P < 0.001$ versus wild type.

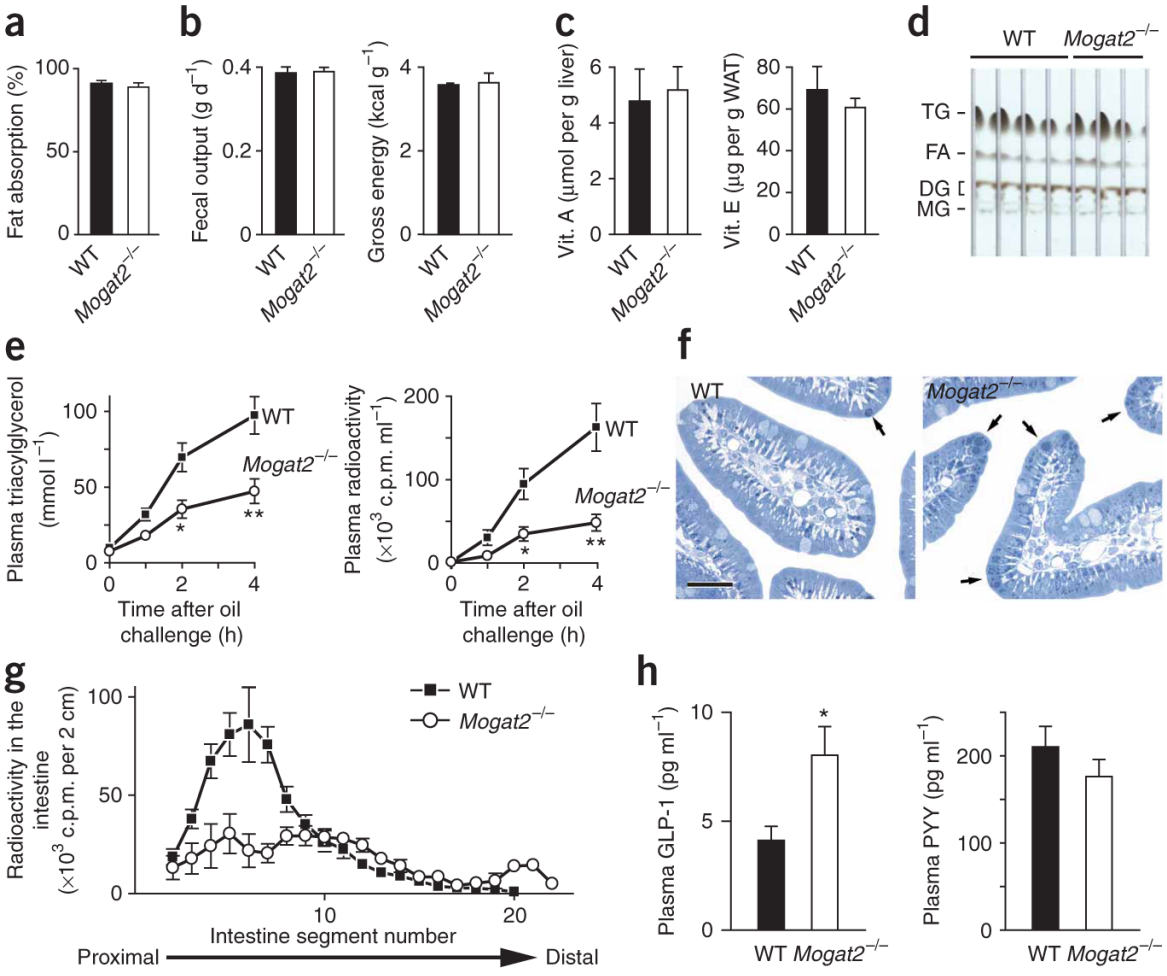

Figure 4.

Fat absorption in MGAT2-deficient mice is quantitatively normal but delayed.

(**a**) Intestinal fat absorption measured in adult mice fed a diet containing 60% of calories from fat. A nonabsorbable fat was used as a marker[13]. Wild-type, $n = 12$; *Mogat2*$^{-/-}$, $n = 14$. (**b**) Output and energy content determined by an adiabatic bomb calorimeter of feces from mice fed a 60% fat diet. Wild-type $n = 9$; *Mogat2*$^{-/-}$, $n = 8$. (**c**) Total amounts of retinol and retinyl esters (Vit. A) in the liver and the levels of α-tocopherol (Vit. E) in the WAT in 10-month-old male wild-type and *Mogat2*$^{-/-}$ mice fed a 60 kcal% fat diet. $n = 6$ mice per group. (**d**) Lipids extracted from the intestinal mucosa of mice fed a high-fat diet for 2 d, resolved by thin-layer chromatography using a two-solvent system[22] and stained with iodine vapor. TG, triacylglycerol; DG, diacylglycerol; MG, monoacylglycerol; FA, fatty acid. (**e**) Plasma triacylglycerol and radioactivity levels in chow-fed female mice after injection of the lipase inhibitor tyloxapol and gavage with olive oil containing ^{14}C-trioleoylglycerol. Wild-type, $n = 7$; *Mogat2*$^{-/-}$ $n = 6$. (**f**) Sections of jejunum from mice fed a high-fat diet. Arrows indicate lipid droplets stained with toluidine blue. Scale bar, 20 μm. (**g**) Altered distribution of dietary triacylglycerol in the small intestine of *Mogat2*$^{-/-}$ mice after an oral challenge of oil. Radioactivity levels 2 h after gavage with oil containing ^{14}C-trioleoylglycerol in intestinal segments of female mice acclimatized to a high-fat diet. $n = 4$ per genotype. (**h**) Postprandial GLP-1 and PYY concentrations in the plasma of chronically high-fat–fed mice. $n = 10$–20 mice per group. Values are means ± s.e.m. *$P < 0.05$ and **$P < 0.001$ versus wild type.